

# Phonon-Wave-Induced Resonance Fluorescence in Semiconductor Nanostructures: Acoustoluminescence in the Terahertz Range

K. J. Ahn, F. Milde, and A. Knorr

*Institut für Theoretische Physik, Nichtlineare Optik und Quantenelektronik, Technische Universität Berlin, Hardenbergstraße 36, PN 7-1 10623 Berlin, Germany*

(Received 10 November 2005; published 8 January 2007)

Acoustic wave excitation of semiconductor quantum dots generates resonance fluorescence of electronic intersublevel excitations. Our theoretical analysis predicts acoustoluminescence, in particular, a conversion of acoustic into electromagnetic THz waves over a broad spectral range.

DOI: [10.1103/PhysRevLett.98.027401](https://doi.org/10.1103/PhysRevLett.98.027401)

PACS numbers: 78.67.Hc, 42.50.Ct, 42.65.Ky, 78.60.Mq

Sonoluminescence (or acoustoluminescence), as discovered in the mid-1930s [1], is the conversion of acoustic energy into electromagnetic radiation [2,3]. Short light bursts can be observed when a bubble trapped in a fluid collapses as it undergoes periodic compression and extension caused by a standing hypersonic acoustic wave. The emission takes only a few picoseconds and has a broad spectral range up to the ultraviolet [4]. The complete physical explanation for this phenomenon is not yet known but its origin is associated to thermal bremsstrahlung [2]. An analog effect was reported in 1980 when cadmium sulfide (CdS) single crystals and alkali halides were exposed to ultrasound waves [5]. Here, the observed luminescence in the visible range is related to intrinsic piezoelectric effects due to lattice defects [6] and was referred to as semiconductor acoustoluminescence (AL).

In this Letter, a conversion mechanism of acoustic energy into THz radiation is proposed for semiconductor nanostructures. Here, similar to a periodic compression of a bubble in a fluid, the quantum confined wave functions of electrons and holes are directly modulated via the band gap modulation due to an externally applied acoustic field. At the same time, the generated electron-hole excitations form a dipole oscillator which emits light. To illustrate our idea, we theoretically analyze a quantized electronic transition in the conduction band of a semiconductor GaAs quantum dot [7,8]. Our focus is on the coherent acoustic excitation of intersublevel transitions in quantum structures due to band off-diagonal contributions in the electron-phonon interaction [9]; cp. Fig. 1: We focus on the light emission spectrum of a quantum dot (QD) intersublevel transition between the lowest quantized electronic states in the conduction band. The transition probability is induced by a monochromatic external acoustic phonon wave. This process supplies a conversion of acoustic into electromagnetic energy (acoustoluminescence) on the nanoscale. Concerning the possibility of the experimental realization, nanomechanical oscillators with a resonance frequency in the range of GHz [10] and hypersonic phononic crystals [11] have been introduced recently.

*Model system.*—In the following we describe our model system for the QD and its interaction with the phonons of

the host material and the quantized photon field: The QD is modeled as a two dimensional disc with a parabolic confinement in the in-plane and an infinitely high potential in the perpendicular direction [12]. Inherent in a two dimensional oscillator model is a degeneracy of the excited states. Therefore, a QD sublevel system with three states in the quantized conduction band ( $|1\rangle$ ,  $|2\rangle$ ,  $|3\rangle$ ,  $E_3 = E_2 > E_1$ ;  $|1\rangle$  contains initially one electron) is driven via a coherent acoustic wave with frequency  $\omega_q$  at wave number  $q$ ; cp. Fig. 1. The optical selection rules allow a transition between the ground state  $|1\rangle$  and both excited states:  $|1\rangle \rightarrow |2\rangle$ ,  $|1\rangle \rightarrow |3\rangle$ , whereas  $|2\rangle \rightarrow |3\rangle$  is optically forbidden. On the other hand, all three states can couple among each other via the acoustic wave (electron-phonon interaction), which induces the possible transitions  $|1\rangle \rightarrow |2\rangle$ ,  $|1\rangle \rightarrow |3\rangle$ , and  $|2\rangle \rightarrow |3\rangle$ . Because of the nondiagonal electron-phonon coupling (see below) and the large energy mismatch between  $\omega_q \approx 1.76$  meV and the electronic transition  $\omega_{12} = 76$  meV (GaAs) [13], off-resonant (many phonon) excitation of the  $|1\rangle \rightarrow |2\rangle$ ,  $|3\rangle$  transition may occur. The acoustically induced electronic excitation is connected to a dipole oscillation (source in Maxwell's equations), and therefore drives the AL.

*Emission spectra.*—The experimental observable related to the steady state emission spectrum  $S(\omega)$  of a single transition  $|i\rangle \rightarrow |1\rangle$  ( $i = 2, 3$ ) can be described in terms of the mean photon number  $n_{\mathbf{k}}$  ( $k = \nu_k/c$ ) [14,15] and is obtained from the Fourier transform ( $\omega = \nu_k$ ) of the

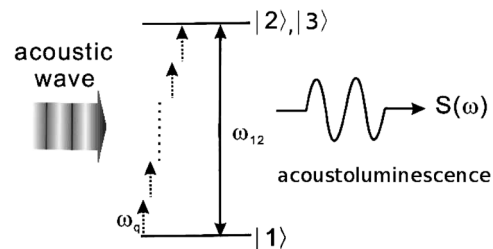


FIG. 1. Scheme for an off-resonant excitation of a quantized conduction band transition  $|1\rangle \rightarrow |2\rangle$ ,  $|3\rangle$  with a transition energy  $\omega_{12}$ , induced by an external acoustic wave with frequency  $\omega_q$ . The emission spectrum is  $S(\omega)$ .

first-order correlation function of the radiation field [16,17]:

$$S_i(\omega, t) \propto \frac{1}{t|g_{1i}(\mathbf{k})|^2} n_{\mathbf{k}}(t), \quad (1)$$

where  $n_{\mathbf{k}} = \langle c_{\mathbf{k}}^\dagger c_{\mathbf{k}} \rangle$  and  $c_{\mathbf{k}}^\dagger (c_{\mathbf{k}})$  denotes the creation (annihilation) operator for a photon of the mode  $\mathbf{k}$  containing a wave vector and a polarization direction  $\mathbf{e}_{\mathbf{k}}$ , while  $t$  is the observation time. Furthermore,  $g_{1i}(\mathbf{k}) = -\mathbf{d}_{1i} \cdot \mathbf{e}_{\mathbf{k}} g_k / \hbar$  [ $g_k = (\hbar \nu_k / 2 \varepsilon_0 V)^{-1/2}$ ] is the electron-photon coupling matrix element [16], where  $\nu_k$  is the frequency of mode  $\mathbf{k}$  and  $V$  the quantization volume. The definition of Eq. (1) holds in the stationary situation when the acoustic pulse envelope is constant in time. In our investigation, the incident acoustic wave is modeled by

$$\Omega(t) = \begin{cases} \exp\left[-\frac{(t-t_0)^2}{\tau^2}\right] \sin(\omega_0 t), & \text{for } t < t_0, \\ \sin(\omega_0 t), & \text{for } t_0 \leq t, \end{cases} \quad (2)$$

with the parameters  $t_0 = 3$  ns and  $\tau = 1$  ns. The spectrum remains unchanged in its shape and is independent on time motivating the notation  $S_i(\omega, t) = S_i(\omega)$  [18]. Because a three-level system must be considered, the total spectrum is given by the sum over both equally possible ( $p_i = 1/2$ ) emission processes [18]:  $S(\omega, t) = \sum_i p_i S_i(\omega, t)$  ( $i = 2, 3$ ). To obtain maximal coupling, we assume that the polarization vector  $\mathbf{e}_{\mathbf{k}}$  of the detected radiation field emitted by the QD is parallel to the dipole direction. The dipole moment  $\mathbf{d}_{1i}$  in the electron-photon coupling constant is calculated from the intersublevel eigenfunctions  $\xi_1(\mathbf{r})$  and  $\xi_i(\mathbf{r})$  ( $i = 2, 3$ ) of the two lowest quantized electronic states in the conduction band:  $\mathbf{d}_{1i} = \int d^3 r \xi_1^*(\mathbf{r}) \mathbf{e} r \xi_i(\mathbf{r})$  [19], with the elementary charge  $e > 0$ , leading to a dipole length calculated as  $|\mathbf{d}_{1i}|/e = \langle 1 | \mathbf{r} | i \rangle \approx 3$  nm. This value is comparable to the experimental value of 3.3 nm measured in Ref. [13]. Note that  $\mathbf{d}_{12} = \mathbf{d}_{13}$ , since the intersublevel eigenfunctions  $\xi_{2/3}(\mathbf{r})$  only differ by a phase factor. Next, to determine  $S(\omega)$ ,  $n_{\mathbf{k}}(t)$  must be computed from its Heisenberg equation of motion.

*Hamiltonian.*—The Hamiltonian of the photon field is given by  $\hat{\mathbf{H}}_{\text{pt}} = \sum_{\mathbf{k}} \hbar \nu_{\mathbf{k}} c_{\mathbf{k}}^\dagger c_{\mathbf{k}}$  and the electron-photon interaction reads  $\hat{\mathbf{H}}_{e\text{-pt}} = \sum_{\lambda, \mu} \sum_{\mathbf{k}} g_{\lambda\mu}(\mathbf{k}) a_{\lambda}^\dagger a_{\mu} (c_{\mathbf{k}} - c_{\mathbf{k}}^\dagger)$ . The operator  $a_{\lambda}^\dagger (a_{\lambda})$  denotes the creation (annihilation) operator of an electron in the state  $\lambda$ ,  $\mu = 1, 2, 3$  in the quantum confined conduction band [16,17]. The free electron field contribution in effective mass approximation is given by  $\hat{\mathbf{H}}_0 = \sum_{\lambda} \varepsilon_{\lambda} a_{\lambda}^\dagger a_{\lambda}$ , where  $\varepsilon_{\lambda}$  denotes the electronic energy of the quantum confined sublevel state  $\lambda$ .

In our semiclassical approach for the electron-phonon interaction, the incident coherent acoustic wave is a classical field, and its interaction with the quantized electrons is described via the deformation potential [20]. The displacement field is given by the externally applied single mode wave  $\mathbf{s}(\mathbf{q}, t) = \mathbf{s}_0 \cos(\mathbf{q} \cdot \mathbf{r} - \omega_q t)$ , where  $\mathbf{s}_0$  denotes the lattice constant variation. Consequently, the electron-phonon interaction Hamiltonian reads [20]

$$\begin{aligned} \hat{\mathbf{H}}_{\text{int}} &= \sum_{\lambda, \mu} \int d^3 r \xi_{\lambda}^*(\mathbf{r}) D_c \mathbf{q} \cdot \mathbf{s}_0(t) \\ &\quad \times \sin(\mathbf{q} \cdot \mathbf{r} - \omega_q t) \xi_{\mu}(\mathbf{r}) a_{\lambda}^\dagger a_{\mu} \\ &= \sum_{\lambda, \mu} \sum_{j=e,o} G_{\lambda\mu}^j(q) \Omega_j(q, t) a_{\lambda}^\dagger a_{\mu}, \end{aligned} \quad (3)$$

where the odd (even) coupling constant matrix element  $G_{\lambda\mu}^{o(e)}(q) = q D_c \mathcal{F}_{\lambda\mu}^{o(e)}(q)$  is defined by the form factor  $\mathcal{F}_{\lambda\mu}^o(q) = \langle \lambda | \sin(\mathbf{q} \cdot \mathbf{R}) | \mu \rangle$  ( $\mathcal{F}_{\lambda\mu}^e(q) = \langle \lambda | \cos(\mathbf{q} \cdot \mathbf{R}) | \mu \rangle$ ) and is evaluated numerically.  $\Omega_o(q, t) = s_0 \cos(\omega_q t)$  and  $\Omega_e(q, t) = s_0 \sin(\omega_q t)$  contain the corresponding temporal oscillation of the acoustic wave.

Numerical calculations for the full three-level system are presented later. However, since the obtained main result, an emission over a broad spectral THz range, is not qualitatively different from the results obtained by a two-level approach, we will present the equations for the more transparent two-level description (ground state  $|1\rangle$  and excited state  $|2\rangle$ ). This can be regarded as an effective level model for the full system. Contrary to the three-level model, here only the sinusoidal part of the incident wave couples to the electronic system, hence the odd part can be neglected and we omit the  $o, e$ : sub- and superscripts.

*Equations of motion.*—Using the total Hamiltonian  $\hat{\mathbf{H}} = \hat{\mathbf{H}}_0 + \hat{\mathbf{H}}_{\text{pt}} + \hat{\mathbf{H}}_{e\text{-pt}} + \hat{\mathbf{H}}_{\text{int}}$ , the Heisenberg equations for the photon number density  $n_{\mathbf{k}}$  and its related hierarchy of coupled equations are calculated [14] in the correlation expansion of the density matrix [17,21]:

$$\partial_t n_{\mathbf{k}}(t) = \partial_t \langle c_{\mathbf{k}}^\dagger c_{\mathbf{k}} \rangle = 2g_{12}(\mathbf{k}) \text{Re}[\langle a_1^\dagger a_2 c_{\mathbf{k}}^\dagger \rangle], \quad (4)$$

$$\begin{aligned} \partial_t \langle a_1^\dagger a_2 c_{\mathbf{k}}^\dagger \rangle &= i\{\nu_k - \tilde{\omega}(q, t)\} \langle a_1^\dagger a_2 c_{\mathbf{k}}^\dagger \rangle + g_{12}(\mathbf{k}) \rho_2(t) \\ &\quad - i\Phi(q, t) \langle A_{\mathbf{k}}^\dagger \rangle(t), \end{aligned} \quad (5)$$

$$\begin{aligned} \partial_t \langle A_{\mathbf{k}}^\dagger \rangle(t) &= \{i\nu_k - \Gamma_1\} \langle A_{\mathbf{k}}^\dagger \rangle(t) + g_{12}(\mathbf{k}) [p(t) - p^*(t)] \\ &\quad - i\Phi(q, t) \{\langle a_1^\dagger a_2 c_{\mathbf{k}}^\dagger \rangle - \langle a_2^\dagger a_1 c_{\mathbf{k}}^\dagger \rangle\}, \end{aligned} \quad (6)$$

$$\begin{aligned} \partial_t \langle a_2^\dagger a_1 c_{\mathbf{k}}^\dagger \rangle &= i\{\nu_k + \tilde{\omega}(q, t)\} \langle a_2^\dagger a_1 c_{\mathbf{k}}^\dagger \rangle + g_{12}(\mathbf{k}) \rho_1(t) \\ &\quad + i\Phi(q, t) \langle A_{\mathbf{k}}^\dagger \rangle(t), \end{aligned} \quad (7)$$

$$\partial_t \rho_2(t) = -\Gamma_1 \rho_2(t) - i\Phi(q, t) \{p(t) - p^*(t)\}, \quad (8)$$

$$\partial_t p(t) = -i\tilde{\omega}(q, t) p(t) - i\Phi(q, t) \{2\rho_2(t) - 1\}. \quad (9)$$

The coupled set of equations contains the photon number  $n_{\mathbf{k}} = \langle c_{\mathbf{k}}^\dagger c_{\mathbf{k}} \rangle$  ( $k = \nu_k/c$ ) which determines the spectrum  $S(\omega)$  [Eq. (1)], the quantum polarization  $\langle a_1^\dagger a_2 c_{\mathbf{k}}^\dagger \rangle$  for simultaneous emission of photons, and an auxiliary operator  $\langle A_{\mathbf{k}}^\dagger \rangle = \langle a_2^\dagger a_2 c_{\mathbf{k}}^\dagger \rangle - \langle a_1^\dagger a_1 c_{\mathbf{k}}^\dagger \rangle$  being a photon-assisted inversion of the electronic transition. Furthermore,  $\rho_{\lambda}(t) = \langle a_{\lambda}^\dagger a_{\lambda} \rangle$  is the occupation density of the state  $\lambda = 1, 2$  and  $p(t) = \langle a_1^\dagger a_2 \rangle$  the intersublevel coherence. As a source

term in each equation of motion, the Rabi frequency  $\Phi(q, t) = G_{12}(q)\Omega(q, t)/\hbar$  of the acoustic pump field is introduced. Compared to the well-known optical Bloch equations of the atomic two-level system [22], the polarization  $p(t)$  (the photon-assisted polarization  $\langle a_1^\dagger a_2 c_k^\dagger \rangle$ ) is coupled to the occupation density  $\rho_2(t)$  (the photon-assisted densities  $\langle a_2^\dagger a_2 c_k^\dagger \rangle$  and  $\langle a_1^\dagger a_1 c_k^\dagger \rangle$ ), and in addition contains a band gap modulation due to the coupling to the acoustic wave via  $\Delta G(q) = G_{22} - G_{11}$  given by a complex frequency including the radiative damping:

$$\tilde{\omega}(q, t) = \omega_{12} + \Delta G(q)\Omega(q, t) - i\Gamma_2. \quad (10)$$

To derive the set of Eqs. (4)–(9), the approximation  $\Gamma_2 = 1/500$  ps  $= \Gamma_1/2$  is used for the derived radiative damping contribution in Markov approximation [16] and additional relaxation contributions. These values do not influence the qualitative features of the obtained spectra, they determine only the linewidth of the individual peaks without changing their qualitative appearance.

*Numerical results.*—First, to discuss the acoustic intersublevel coupling strength, a deformation potential of the conduction band  $D_c = -14.6$  eV [20] and a maximal crystal ion's elongation  $s_0$  of 0.5% of the lattice constant in equilibrium ( $a_{\text{GaAs}} \approx 0.5$  nm [23]) are used. The coupling constants  $G_{12}(q)$  are calculated as a function of the wave number  $q$ ; cp. Fig. 2. The calculation predicts a coupling strength in the meV range for 0.5% elongation of the lattice constant  $a_{\text{GaAs}}$ . An inspection of the coupling constants  $G_{12}(q)$  and  $\Delta G(q)$  shows that a specific wave vector  $q_0$  exists where the gap modulation  $\Delta G(q_0)$  Eq. (10) vanishes. At the same time, the direct coupling  $G_{12}(q_0)$  is close to its maximal value. Thus, an optimal excitation can be achieved by choosing the wave vector as  $q_0 = \omega_0/c_s \approx 0.524$  nm $^{-1}$  where the polarization is not frequency modulated [ $\Delta G(q) = 0$  in Eq. (9)]. In this case, the equations are close to an ideal two-level system in quantum optics [16]. The intersublevel coupling strength  $G_{12}(q)$  as well as typical phonon energies  $\omega_q$  of several meV [24] are small compared with a typical intersublevel transition energy of

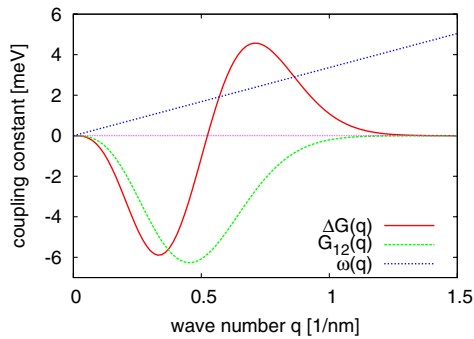


FIG. 2 (color online). Electron-phonon coupling constants as a function of wave number: For  $s_0 = 0.005a_{\text{GaAs}}$ , the interlevel coupling  $G_{21}(q)$ , the gap modulation  $\Delta G(q)$ , and the dispersion relation in GaAs  $\omega(q) = c_s q$  are plotted as a function of the wave number  $q$ .

several tens of meV in QDs [13]. Therefore, the acoustically induced AL dynamics are in the well off-resonant regime. Next, the numerical evaluation of the fluorescence spectra is presented. To discuss a broad range of the AL emission dynamics, we focus on (i) a weak excitation (linear AL) and (ii) a strong excitation (nonlinear AL).

(i) For weak excitation power (maximal deflection of the lattice constant  $s_0 = 10^{-4}a_{\text{GaAs}}$ ), the AL power spectrum in Fig. 3 shows a Lorentzian peak at the phonon frequency of the acoustic wave  $\omega_0 = 1.76$  meV, i.e., in the THz regime (1 meV  $\hat{=}$  2.42 THz): Because of the large detuning and a small spectral width of the driving field compared with  $\omega_{12}$ , the intersublevel dipole oscillator reacts with the driving phonon frequency  $\omega_0$ . To calculate the stationary spectrum, which is proportional to the photon number density [25],  $\langle a_1^\dagger a_2 c_k^\dagger \rangle$  [see Eq. (4)] must be known.

For an analytical insight, we assume that all time derivatives of photon-assisted electronic densities are zero (stationary situation) and obtain [16] ( $\omega = \nu_k$ ):

$$S(\omega) \propto \frac{\Gamma_1 \rho_2}{(\omega - \omega_0)^2 + \Gamma_1^2}, \quad (11)$$

which states that the radiation occurs at the frequency  $\omega_0$  of the acoustic wave and  $\rho_2$  is a stationary value.

(ii) For a strong driving acoustic field, multiple phonon absorption is possible. Here, we investigate a set of coupling strengths up to  $G_{12}(q_0) \approx -15$  meV, which corresponds to a maximal deflection  $s_0 = 0.01a_{\text{GaAs}}$  and is a fifth of the transition frequency  $\hbar\omega_{12}$  at the chosen wave vector  $q_0 = 0.52$  nm $^{-1}$ . Figure 4 shows the AL spectra  $S(\omega)$  of the full three-level calculations for increasing excitation strength  $s_0 = 0.001a_{\text{GaAs}}$ ,  $s_0 = 0.005a_{\text{GaAs}}$ , and  $0.01a_{\text{GaAs}}$ . The solution of our equations is comparable to a highly nonlinear radiation spectrum of an effective two-level system driven off-resonantly by an intense optical field: the spectra consist of two series of peaks [26–28]: higher-order harmonics (HOH) at the odd multiples  $(2n + 1)\omega_L$  of the driving field frequency  $\omega_L$  and hyper Raman (HR) peaks at the even multiples  $2n\omega_L \pm \tilde{\omega}_g$  around the renormalized gap frequency  $\tilde{\omega}_g$ . For a sufficiently strong phonon field intensity, both series can overlap and interfere

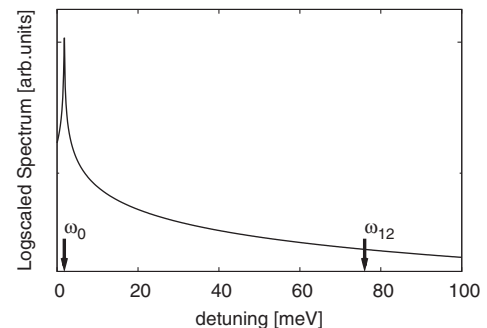


FIG. 3. Acoustoluminescence emission spectrum for weak coupling. The excitation frequency  $\omega_0 = 1.76$  meV and the transition frequency  $\omega_{12} = 76$  meV are marked.

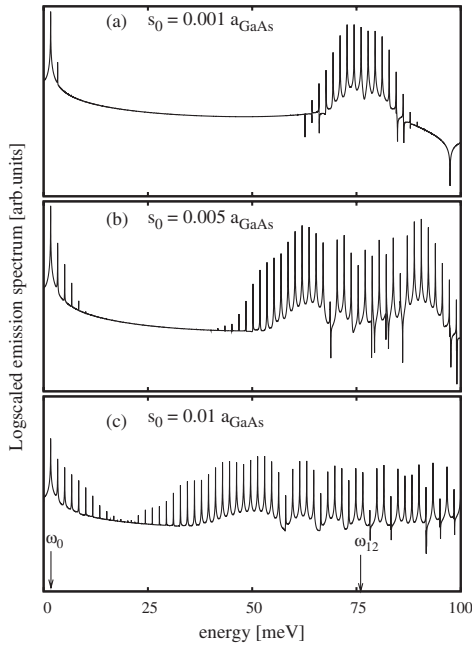


FIG. 4. Emission spectra in the strong coupling regime for a three-level system with a deflection of (a) 0.1%, (b) 0.5%, and (c) 1% of the lattice constant  $a_{\text{GaAs}}$ .

with each other, resulting in a constant spectral domain, referred to as a plateau region [29]. For all spectra in Fig. 4, we obtain an enhancement of the AL around the electronic transition ( $\omega_{12} = 76$  meV). This enhancement results from the strong oscillator strength at the intersublevel resonance which is off-resonantly excited via multiphonon processes. HOH emission at all odd multiples of the phonon energy  $\omega_0$  can be found. While only the HOH peaks exist at low excitation [Fig. 4(a)], some HR peaks emerge and the plateau formation can be found at higher excitations. In conclusion, this Letter illustrates the possibility of luminescence in the THz regime due to the conversion of incident acoustic into electromagnetic energy, including higher-order harmonics, for a semiconductor nanostructure. A further refinement of the model, in particular, for the strong coupling case, should include further states and nonharmonic effects up to possible melting dynamics.

The authors would like to thank Alfred Leitenstorfer, Thomas Dekorsy, Anton Plech (Konstanz), and Stephen Hughes (Queen's University, Kingston) for helpful discussions. This work has been financially supported by the DFG through Grant No. Sfb296.

- [1] H. Frenzel and H. Schultes, *Z. Phys. Chem. B* **27**, 421 (1934).  
 [2] R. Toegel, S. Hilgenfeldt, and D. Lohse, *Phys. Rev. Lett.* **88**, 034301 (2002).

- [3] D. Lohse, *Nature (London)* **434**, 33 (2005).  
 [4] B. P. Barber, C. C. Wu, R. Lofstedt, P. H. Roberts, and S. J. Putterman, *Phys. Rev. Lett.* **72**, 1380 (1994).  
 [5] I. V. Ostrovskii, A. K. Rozhko, and V. N. Lysenko, *Sov. Tech. Phys. Lett.* **5**, 377 (1979).  
 [6] I. V. Ostrovskii, *Sov. Phys. JETP* **34**, 446 (1981).  
 [7] L. Bányai and S. W. Koch, *Semiconductor Quantum Dots* (World Scientific Publishing, Singapore, 1993).  
 [8] D. Bimberg, M. Grundmann, and N. Ledentsov, *Quantum Dot Heterostructures* (John Wiley & Sons, Chichester, 1999).  
 [9] I. Waldmüller, J. Förstner, S.-C. Lee, A. Knorr, M. Woerner, K. Reimann, R. A. Kaindl, T. Elsaesser, R. Hey, and K. H. Ploog, *Phys. Rev. B* **69**, 205307 (2004).  
 [10] A. Gaidarzhy, G. Zolfagharkhani, R. L. Badzey, and P. Mohanty, *Phys. Rev. Lett.* **94**, 030402 (2005).  
 [11] T. Gorishnyy, C. K. Ullal, M. Maldovan, G. Fytas, and E. L. Thomas, *Phys. Rev. Lett.* **94**, 115501 (2005).  
 [12] M. Sugawara, *Phys. Rev. B* **51**, 10743 (1995).  
 [13] S. Sauvage, P. Boucaud, J. M. Gerard, and V. Thierry-Mieg, *Phys. Rev. B* **58**, 10562 (1998).  
 [14] K. J. Ahn, J. Förstner, and A. Knorr, *Phys. Rev. B* **71**, 153309 (2005).  
 [15] M. Richter, M. Schaarschmidt, A. Knorr, W. Hoyer, J. V. Moloney, E. M. Wright, M. Kira, and S. W. Koch, *Phys. Rev. A* **71**, 053819 (2005).  
 [16] M. O. Scully and M. S. Zubairy, *Quantum Optics* (Cambridge University Press, Cambridge, 1997).  
 [17] M. Kira, F. Jahnke, W. Hoyer, and S. W. Koch, *Prog. Quantum Electron.* **23**, 189 (1999).  
 [18] W. Vogel and D. Welsch, *Quantum Optics An Introduction* (Wiley-VCH, Berlin, 2001).  
 [19] P. Borri, W. Langbein, U. Woggon, V. Stavarache, D. Reuter, and A. D. Wieck, *Phys. Rev. B* **71**, 115328 (2005).  
 [20] B. Krummheuer, V. M. Axt, and T. Kuhn, *Phys. Rev. B* **65**, 195313 (2002).  
 [21] I. Waldmüller, J. Förstner, and A. Knorr, in *Nonequilibrium Physics at Short Time Scales* (Springer-Verlag, Berlin, 2004).  
 [22] L. Allen and J. H. Eberly, *Optical Resonance and Two-Level Atoms* (Dover Publications, New York, 1987).  
 [23] *Physics of Group IV Elements and III-V Compounds*, edited by O. Madelung, Landolt-Börnstein, New Series, Group III Vol. 17 (Springer, Berlin, 1982), Pt. a.  
 [24] P. Borri, W. Langbein, S. Schneider, U. Woggon, R. L. Sellin, D. Ouyang, and D. Bimberg, *Phys. Rev. Lett.* **87**, 157401 (2001).  
 [25] B. Benaud, R. M. Whitley, and C. R. Stroud, Jr., *J. Phys. B* **10**, 19 (1977).  
 [26] H. C. Torrey, *Phys. Rev.* **76**, 1059 (1949).  
 [27] S. H. Autler and C. H. Townes, *Phys. Rev.* **100**, 703 (1955).  
 [28] P. P. Corso, L. LoCascio, and F. Persico, *J. Mod. Opt.* **44**, 819 (1997).  
 [29] P. P. Corso, L. LoCascio, and F. Persico, *Phys. Rev. A* **58**, 1549 (1998).